



Virtual Experiments on Coarse-Grained Soil Using X-Ray CT and Finite Element Analysis

Mohamed Abdennadher¹

¹ Hamburg University of Technology, Schellerdamm 22-24, 21079 Hamburg, Germany
mohamed.abdennadher@tuhh.de

Abstract. Digital rock physics combines imaging and numerical techniques to study the mechanical properties of granular materials without extensive physical experiments. This paper introduces a workflow for processing X-Ray Computed Tomography (CT) data and using it in numerical simulations, demonstrated through the compression of coarse-grained soil. High-resolution CT scans capture the 3D structure of soil, with noise reduction, binarization, and segmentation isolating individual particles. Particle shapes and size distributions are extracted and used to create finite element models comprising approximately 500 particles. The models are meshed with varying fineness to balance computational efficiency and shape accuracy, with finer meshes at particle surfaces and coarser meshes internally. Numerical simulations of uniaxial compression exhibit qualitative agreement with laboratory data, though the simulation predicts higher stiffness. Frictional interactions - sliding, rotation, and rolling - are identified as dominant deformation mechanisms. This workflow demonstrates an efficient method for integrating CT data into simulations, providing a foundation for future improvements to better align simulations with laboratory-scale experiments.

Keywords: Digital Rock Physics, Finite Element Analysis, X-Ray Computed Tomography.

1 Introduction

Understanding the mechanical behavior of granular materials, such as coarse-grained soils, is fundamental in geotechnical engineering and related fields. Traditional laboratory testing methods, while accurate, often require significant time and resources, especially when investigating complex material behaviors under varied conditions. Recent advancements in digital rock physics have introduced innovative techniques that combine high-resolution imaging with computational simulations [1-5], offering a powerful alternative to physical experiments.

This study explores the potential of X-Ray Computed Tomography (CT) and finite element analysis (FEA) to establish a virtual testing framework for coarse-grained soils. By capturing the three-dimensional structure of soil at the particle level, CT imaging provides detailed insights into particle morphology and interactions. The

subsequent use of FEA enables the simulation of soil behavior under compression, offering a means to analyze stress distribution and deformation patterns with high precision.

The motivation for this research lies in the need to enhance efficiency and scalability in soil mechanics studies while maintaining accuracy. By integrating CT imaging and FEA, this work aims to validate virtual testing as a reliable method for predicting soil behavior and uncovering critical insights into the influence of inter-particle interactions. This approach has the potential to reduce dependence on physical laboratory tests, advancing the field of geomechanics through digital innovation.

2 X-Ray Computed Tomography (CT)

X-Ray Computed Tomography (CT) has emerged as an indispensable tool in geomechanics, offering a non-destructive way to study the internal structure and behavior of granular materials like soils and rocks. Initially developed for medical imaging, CT technology has been adapted to geomechanical research, allowing the visualization and analysis of particle morphology, pore spaces, and mechanical interactions within materials under stress. By generating high-resolution three-dimensional images, CT provides insights that traditional experimental methods often cannot achieve.

The CT process, illustrated in Fig. 1, involves placing a sample on a rotating stage while an X-ray source emits beams that penetrate the material. A detector records these beams after they pass through the sample, creating a series of two-dimensional radiographic images. Computational algorithms reconstruct these projections into a 3D model, revealing the internal structure of the material.

CT technology has been widely used in geomechanics to analyze particle shapes, sizes, and orientations, examine pore structures, visualize deformation patterns under loading, and monitor crack propagation in rocks. Despite its advantages, CT does have limitations. High-resolution scans are restricted to small samples, making it challenging to extrapolate findings to field-scale conditions. Materials with similar densities or compositions may lack sufficient contrast for accurate segmentation, and noise or artifacts from the imaging process can affect the quality of results. Additionally, CT equipment is expensive, and high-resolution imaging can be time-intensive, requiring careful preprocessing and calibration to ensure accuracy.

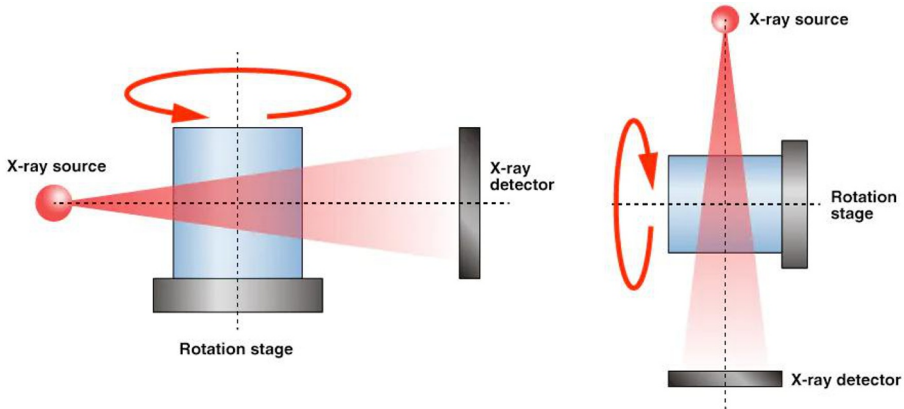


Fig. 1. Illustration of the CT process: The sample is placed on a rotating stage and scanned by an X-ray source, which emits beams that penetrate the material. A detector captures the transmitted X-rays to produce multiple 2D projections. Figure adapted from [6].

3 Particle Shape Extraction from CT Imaging Data

The extraction of particle shapes from CT imaging data is achieved through a systematic process comprising filtering, binarization, and segmentation. These steps are essential for isolating individual particles with high accuracy. Fig. 2 illustrates this workflow: the left panel shows the raw CT data, the middle panel represents the intermediate stages following filtering, binarization, and segmentation, and the right panel displays the final rendered particles.

The raw CT data contains noise and imaging artifacts that must be removed to ensure accurate segmentation. A median noise filter is applied as a preprocessing step, which suppresses high-frequency noise while preserving particle boundaries. This filtering step enhances the clarity of the particle structures without introducing distortion. Following noise reduction, the images are binarized to differentiate between particles and their surrounding air. While CT data often includes multiple phases, such as particles, water, and air, the current study involves only two phases: particles and air. A global intensity threshold is applied to generate a binary image, assigning voxels to either the particle or air phase. The segmented binary image is processed using the watershed algorithm to isolate individual particles. This algorithm conceptualizes the binary image as a topographical surface, where voxel intensities correspond to elevation. Local intensity minima are identified as seed points, and the algorithm incrementally "floods" the surface, assigning voxels to their nearest seed. This approach ensures accurate separation of particles, even in cases where they are in contact or partially overlapping. To refine the segmentation, a distance transform is computed, providing a gradient map that aids in accurately delineating particle boundaries. The resulting segmented particles are then labeled and rendered.

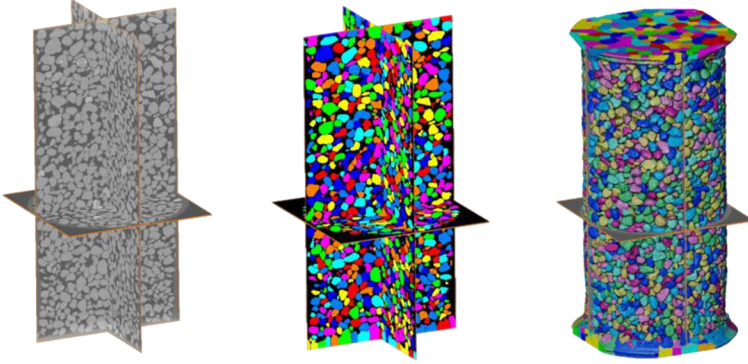


Fig. 2. Workflow for particle shape extraction from CT imaging data. The left panel shows the raw CT data, the middle panel illustrates the intermediate processing stages, including filtering, binarization, and segmentation, and the right panel displays the final rendered particles after segmentation.

4 Meshing and Sample Creation

After particle rendering, meshing is required for numerical simulations. The mesh must balance computational efficiency with accurate particle shape representation. A fine mesh preserves surface details, which is essential for capturing inter-particle interactions, but increases computational demands, limiting the number of particles in a simulation. A practical solution is to vary mesh fineness: the outer particle surface is finely meshed to retain shape accuracy, while the interior uses a progressively coarser mesh to reduce computational cost. This method, while efficient, introduces stiffness artifacts in the particle's interior due to reduced degrees of freedom, potentially affecting deformation behavior. Such trade-offs must be considered when interpreting simulation results.

Once the particles have been meshed, they are assembled into a sample for numerical simulations. The sample is generated by randomly positioning and orienting the particles inside a rigid cylindrical container, into which they are dropped under gravity. During this process, the particles are temporarily treated as rigid bodies to accelerate the settling phase and avoid excessive computational costs associated with early-stage rearrangements. Once the sample is settled, the rigid cylinder is retained in the numerical simulations to provide lateral confinement. This ensures that no displacement occurs in directions perpendicular to the compression axis, enforcing uniaxial deformation.

Figure 3 shows the final cylindrical specimen, which consists of approximately 500 particles, with a height of around 5 mm and a diameter of 3 mm. Due to computational constraints, it is not feasible to simulate real laboratory experiments, which involve millions of particles. However, to ensure that the reduced model remains representative of the real material, the particle size distribution in the simulation is designed to closely match that of the experimental sample.

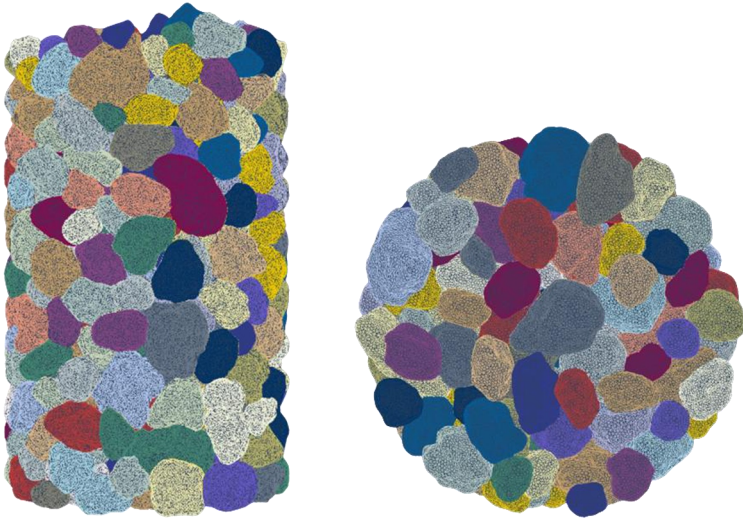


Fig. 3. Cylindrical specimen containing approximately 500 particles, with a height of 5 mm and a diameter of 3 mm, used for numerical simulations. The specimen is created by combining meshed particles to form a representative sample for granular material.

5 Numerical Simulation

Once the specimen has been created, it can be saved and used for numerical simulations. The finite element simulations in this study were conducted using Abaqus 2023, employing the general contact algorithm to model inter-particle interactions. The material parameters used in the simulation correspond to Hamburger Sand, with values taken from [7], which is the same sand used in the laboratory experiments.

Figure 4 presents an example of a uniaxial compression test performed on a specimen composed of meshed particles. The figure illustrates the stress distribution within the compressed sample, with distinct force chains through which the load is transmitted. These force chains highlight the network of particle contacts that bear the majority of the applied load, providing insights into the mechanics of granular materials under compression.

On the right side of Figure 4, a comparison between the numerical simulation and the laboratory experiment is shown, depicting the stress-strain relationship. While both exhibit qualitatively similar trends, a clear quantitative mismatch is evident: the simulation predicts a stiffer response than observed in the actual laboratory test. This discrepancy can be attributed to several factors. First, as previously discussed, the meshing strategy—particularly the use of a coarser mesh in the particle interiors—introduces artificial stiffness, affecting the deformation behavior. Second, scaling effects are significant, as the laboratory experiment involves millions of particles, whereas the numerical model represents the material using only around 500 particles, potentially altering collective behavior. Lastly, numerical issues arising from the cho-

sen meshing strategy and boundary conditions may also contribute to the observed differences.

These findings indicate that while the presented workflow successfully captures general trends in granular material behavior, it requires further refinement to achieve better quantitative agreement with experimental results. The author acknowledges that this workflow, in its current state, does not provide a fully reliable quantitative prediction of laboratory-scale behavior. Future studies are necessary to fine-tune the approach, addressing meshing strategies, material parameter calibration, and upscaling methodologies to bridge the gap between numerical and experimental outcomes.

Fig. 5 illustrates the ratio between frictional energy dissipation and energy dissipation due to strain as a function of strain. The results show that, throughout the compression process, a significant portion of the total energy dissipation originates from frictional interactions at inter-particle contacts, rather than from the elastic deformation of individual grains. This indicates that under low to intermediate confining pressures, the primary deformation mechanisms are sliding, rotation, and rolling at these contacts. As the confining pressure increases, however, this trend shifts. The proportion of frictional dissipation decreases, and deformation mechanisms become more influenced by grain compression and rearrangement. At higher pressures, particles experience increased contact forces, leading to greater inelastic deformation and possibly particle breakage.

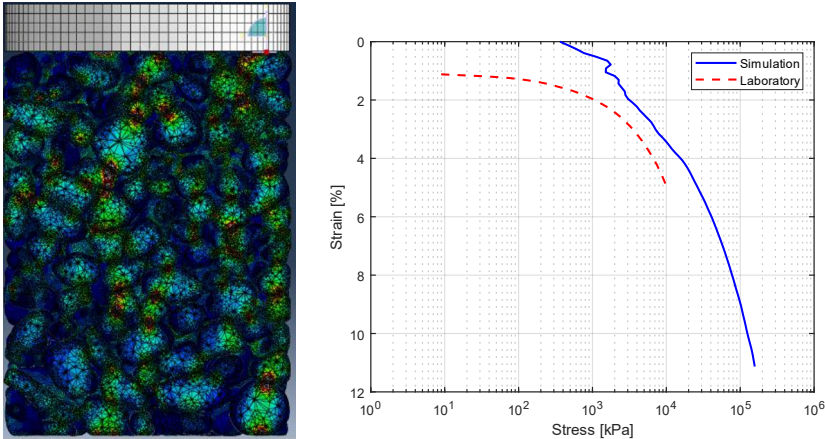


Fig. 4. Left: Stress distribution in a numerically simulated uniaxial compression test, showing force chains and stress concentrations in the specimen. Right: Comparison of the stress-strain relationship between the numerical simulation and laboratory experiment, illustrating similar trends but a higher stiffness in the simulation

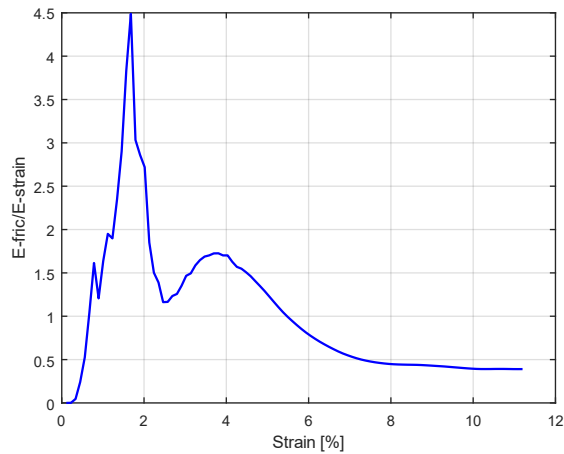


Fig. 5. Ratio of frictional energy dissipation to total energy dissipation as a function of strain.

6 Conclusion

This study presents a workflow for integrating X-Ray Computed Tomography (CT) data and finite element analysis (FEA) to investigate the mechanical behavior of coarse-grained soils. The proposed methodology demonstrates how high-resolution CT scans can capture the internal morphology of soil particles, and how this data can be processed and used to create meshed particle models for numerical simulations. Through a uniaxial compression, we validated the approach by comparing the simulation results with laboratory experiments, revealing similar stress-strain trends despite certain discrepancies in stiffness predictions. The findings highlight the potential and limitations of virtual testing in geomechanics. The simulations revealed that frictional interactions, including sliding, rotation, and rolling at inter-particle contacts, are dominant deformation mechanisms under low to intermediate confining pressures. These insights, which are challenging to achieve with physical experiments alone, underscore the strength of numerical simulations in providing detailed information about soil behavior. However, limitations, such as artificial stiffness introduced by coarse particle meshes and the reduced particle count in simulations, emphasize the need for further refinement of the methodology. Ultimately, this work establishes a foundational framework for processing CT data and incorporating it into numerical simulations. While the primary goal was to present and validate the workflow, future research should focus on improving the scalability and accuracy of these simulations, bridging the gap between numerical and experimental results, and extending the application of this approach to more complex soil behaviors and loading conditions.

References

1. Thakur, M.M., Penumadu, D.: Triaxial compression in sands using FDEM and micro-X-ray computed tomography. *Computers and Geotechnics* 124, 103638 (2020).
2. Nadimi, S., Fonseca, J.: Image-based simulation of one-dimensional compression tests on carbonate sand. *Meccanica* 54(4), 697–706 (2019) .
3. Turner, A.K., Kim, F.H., Penumadu, D., Herbold, E.B.: Meso-scale framework for modeling granular material using computed tomography. *Computers and Geotechnics* 76, 140–146 (2016).
4. Nadimi, S., Fonseca, J., Andò, E., Viggiani, G.: A micro finite-element model for soil behaviour: experimental evaluation for sand under triaxial compression. *Géotechnique* 70(10), 931–936 (2020).
5. Turner, A.K., Sharma, A., Penumadu, D., Herbold, E.B.: Finite element analyses of single particle crushing tests incorporating computed tomography imaging and damage mechanics. *Computers and Geotechnics* 115, 103158 (2019).
6. Matsusada Precision, <https://www.matsusada.com/column/words-ct.html>, last accessed 2025/01/09.
7. Kanitz, M.: Experimental and numerical investigation of particle-fluid systems in geotechnical engineering. Hamburg University of Technology (2021). <http://hdl.handle.net/11420/9830>.

Open Access This chapter is licensed under the terms of the Creative Commons Attribution-NonCommercial 4.0 International License (<http://creativecommons.org/licenses/by-nc/4.0/>), which permits any noncommercial use, sharing, adaptation, distribution and reproduction in any medium or format, as long as you give appropriate credit to the original author(s) and the source, provide a link to the Creative Commons license and indicate if changes were made.

The images or other third party material in this chapter are included in the chapter's Creative Commons license, unless indicated otherwise in a credit line to the material. If material is not included in the chapter's Creative Commons license and your intended use is not permitted by statutory regulation or exceeds the permitted use, you will need to obtain permission directly from the copyright holder.

